View metadata, citation and similar papers at core.ac.uk
brought to you by CORE
provided by University of Regensburg Publication Server

PHYSICAL REVIEW B **87**, 115202 (2013)

Radiation-enhanced self- and boron diffusion in germanium

S. Schneider and H. Bracht*
Institute of Materials Physics, Westfälische Wilhelms-Universität Münster, D-48149 Münster, Germany

J. N. Klug
RUBION, Ruhr-Universität Bochum, D-44780 Bochum, Germany

J. Lundsgaard Hansen and A. Nylandsted Larsen
Department of Physics and Astronomy, University of Aarhus, DK-8000 Aarhus, Denmark

D. Bougeard
Institute of Experimental and Applied Physics, University of Regensburg, 93040 Regensburg, Germany

E. E. Haller
Lawrence Berkeley National Laboratory and University of California, Berkeley, California 94720, USA
(Received 10 December 2012; revised manuscript received 6 February 2013; published 11 March 2013)

We report experiments on proton radiation-enhanced self- and boron (B) diffusion in germanium (Ge) for temperatures between 515 °C and 720 °C. Modeling of the experimental diffusion profiles measured by means of secondary ion mass spectrometry is achieved on the basis of the Frenkel pair reaction and the interstitialcy and dissociative diffusion mechanisms. The numerical simulations ascertain concentrations of Ge interstitials and B-interstitial pairs that deviate by several orders of magnitude from their thermal equilibrium values. The dominance of self-interstitial related defects under irradiation leads to an enhanced self- and B diffusion in Ge. Analysis of the experimental profiles yields data for the diffusion of self-interstitials (I) and the thermal equilibrium concentration of BI pairs in Ge. The temperature dependence of these quantities provides the migration enthalpy of I and formation enthalpy of BI that are compared with recent results of atomistic calculations. The behavior of self- and B diffusion in Ge under concurrent annealing and irradiation is strongly affected by the property of the Ge surface to hinder the annihilation of self-interstitials. The limited annihilation efficiency of the Ge surface can be caused by donor-type surface states favored under vacuum annealing, but the physical origin remains unsolved.

DOI: 10.1103/PhysRevB.87.115202 PACS number(s): 61.72.uf, 61.72.jj, 66.30.H−, 66.30.J−

I. INTRODUCTION

During the last decade, germanium (Ge) has received renewed attention as semiconductor material for integrated circuits.[1–3] This is due to the advantageous electron and hole mobilities that are higher than those of silicon (Si).[4] Full integration of Ge in electronic devices requires a comprehensive understanding of the processes that affect the doping and diffusion at the atomic scale.

Fundamental research on diffusion in silicon performed over the past decades has revealed the significance of both vacancies (V) and self-interstitials (I) in self- and dopant diffusion (see, e.g., Ref. 5 and references therein). In the case of Ge, fundamental studies on diffusion clearly reveal the dominance of V in self- and dopant diffusion under thermal equilibrium conditions.[6–10] This, in particular, holds for the diffusion of n-type (phosphorus, arsenic, and antimony)[10] and p-type (aluminium, gallium, indium)[11–15] dopants. No evidence of I has been found in conventional self-diffusion experiments.[16] This is consistent with theoretical predictions that reveal a formation enthalpy of I being 1–2 eV higher than for V.[17–24] However, recent experiments on self- and dopant diffusion in Ge under proton irradiation indicate the dominance of I rather than of V.[25–29] This observation is of scientific and technologic significance as it provides not only information about the interaction of dopant atoms with I, but also insight into the property of the Ge surface that supports an I supersaturation and V thermal equilibrium under irradiation. The impact of the Ge surface is highly relevant as it will offer strategies to control diffusion in and doping of Ge.

This work presents a detailed description of self- and boron (B) diffusion in Ge under *in situ* proton irradiation. It is evidenced that I's dominate self- and dopant diffusion under irradiation, whereas the vacancy concentration stays close to thermal equilibrium. Properties deduced for I and BI pairs on the basis of a common set of diffusion reaction equations and model parameters support recent theoretical calculations for the migration energy of I (Ref. 30) and formation energy of BI pairs.[31,32]

II. EXPERIMENT

For our experiments of Ge self-diffusion under proton irradiation, we used three different structures Nos. 1 to 3 with alternating isotopically enriched ^{70}Ge (96% enrichment) and natural Ge (^{nat}Ge) layers grown by means of molecular beam epitaxy (MBE) on (100)-oriented single-crystalline Ge wafers (>30 Ω cm). Structure No. 1 consists of five alternating bilayers of ^{70}Ge(100 nm)/^{nat}Ge(100 nm) with a top 300-nm-

 ©2013 American Physical Society

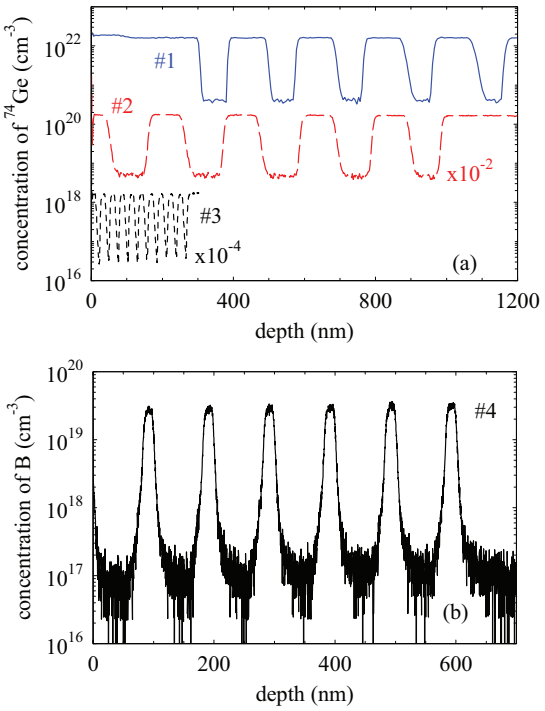

FIG. 1. (Color online) (a) SIMS concentration profiles of ^{74}Ge for the three (Nos. 1 to 3) ^{70}Ge/^{nat}Ge isotope multilayer structures grown by means of MBE and used in this work for studying self-diffusion in Ge under proton irradiation. For clarity, the profiles of Nos. 2 and 3 were shifted by a factor of 10^{-2} and 10^{-4}, respectively. (b) SIMS concentration profile of B in Ge for a delta B-doped multilayer structure grown by MBE. This structure served for experiments of B diffusion under proton irradiation. See Sec. II for more details on the Ge-isotope and B-doped multilayer structures.

thick natural Ge layer. The topmost near-surface 100-nm-thick natural Ge layer is amorphous and grown on 200-nm-thick crystalline Ge. This sample structure was designed for studying the simultaneous diffusion of self- and dopant atoms, whereto the dopant of interest was implanted into the top amorphous layer.[8] Structure No. 2 consists of five alternating ^{70}Ge(100 nm)/^{nat}Ge(100 nm) bilayers with a top 50-nm-thick natural crystalline Ge layer. Finally, structure No. 3 is characterized by 10 alternating ^{70}Ge(15 nm)/^{nat}Ge(15 nm) Ge bilayers with a 15-nm-thick ^{nat}Ge top layer. The concentration profiles of ^{74}Ge recorded by means of time-of-flight secondary ion mass spectrometry (TOF-SIMS) are illustrated in Fig. 1(a). The profiles illustrate the difference in the ^{74}Ge isotope between ^{nat}Ge and ^{70}Ge layers. Structures 1 to 3 are well suited to study the self-diffusion as a function of distance from the surface. The thicker isotope structures serve for diffusion anneals at higher temperatures as the thinner structure would be already homogeneously broadened by conventional furnace annealing at such temperatures.

Experiments on the diffusion of B under proton irradiation were performed with MBE grown B-doped Ge samples that consist of six 25-nm-thick B-doped Ge layers separated by 100-nm undoped natural Ge. A SIMS analysis of the B-doped multilayer structure No. 4 is illustrated in Fig. 1(b).

Samples with lateral dimensions of 4×4 mm^2 were cut from the as-grown Ge wafers, thinned to a thickness of $30(\pm 5)$ μm, and polished with Nalco 2360 (Bucher AG, Switzerland) or Köstrosol 3550 (Chemiewerk Bad Köstritz, Germany) to obtain a scratch-free and specular surface on the back. The samples were mounted on a graphite holder and fixed via a graphite plate with a circular aperture of 3 mm in diameter. In this way, the outer part of the Ge sample was covered with graphite and not exposed to the proton beam. The graphite holder was placed on a boron nitride heating plate that enables heating of the Ge sample during irradiation. The temperature was controlled with a thermocouple mounted 1 mm below the sample in the graphite holder. The whole sample holder was attached to a high-vacuum chamber. Protons of 2.5 MeV were supplied via a beam line from a dynamitron accelerator of the RUBION Bochum. The beam was defocused and swept to achieve a homogeneously irradiated circular area with a diameter of about 1 cm. An electron suppression, which consists of a negatively biased (600-V) screen, ensures that the measurement of the proton current is not hampered by secondary electrons. Proton irradiations were performed for temperatures between 515 °C and 720 °C at proton fluxes varying between 0.8 and 2.5 μA. The high energy of the protons assures that the protons penetrate through the entire Ge sample as ascertained by simulations of the "stopping and range of ions in matter"[33] (SRIM). After annealing under proton irradiation, the concentration profiles of ^{74}Ge and B were measured with TOF-SIMS. The depth of the SIMS craters was determined using an optical profilometer. Cross-section transmission electron microscopy was performed to check the crystalline quality of samples before and after annealing.

III. RESULTS

Figures 2(a)–2(c) show concentration profiles of ^{74}Ge obtained after concurrent diffusion annealing and proton irradiation of samples 1 to 3, respectively. The short-dashed profile in Fig. 2(c) illustrates the ^{74}Ge distribution of the as-grown isotope structure No. 3. The long dashed profile represents self-diffusion under thermal equilibrium beneath the covered, not proton-exposed, part of sample No. 3. A radiation-enhanced diffusion is clearly evident. The self-diffusion profiles obtained for the covered part of the sample served as a calibration of the temperature established during irradiation. Beforehand, we checked the quality of the Ge isotope structures by thermal anneals without proton exposure and verified the literature data on Ge self-diffusion.[6,16]

In contrast to self-diffusion of silicon under irradiation,[34] the ^{74}Ge self-diffusion profiles do not reveal an increasing self-diffusion with increasing penetration depth. This holds for both the thick (Nos. 1 and 2) and thin (No. 3) isotope structures. Usually, a depth dependence of self-diffusion under irradiation is expected because the surface of a material is believed to be an efficient sink for native defects.[34] Hence, the native defect concentration established under irradiation should decrease near the surface and with it the self-diffusion. The absence of any significant gradient in self-diffusion with depth indicates a limited probability of defect annihilation at the Ge surface. Transmission electron microscopy (TEM) investigations reveal the single-crystalline quality of the Ge sample after irradiation, i.e., no extended defects were found.

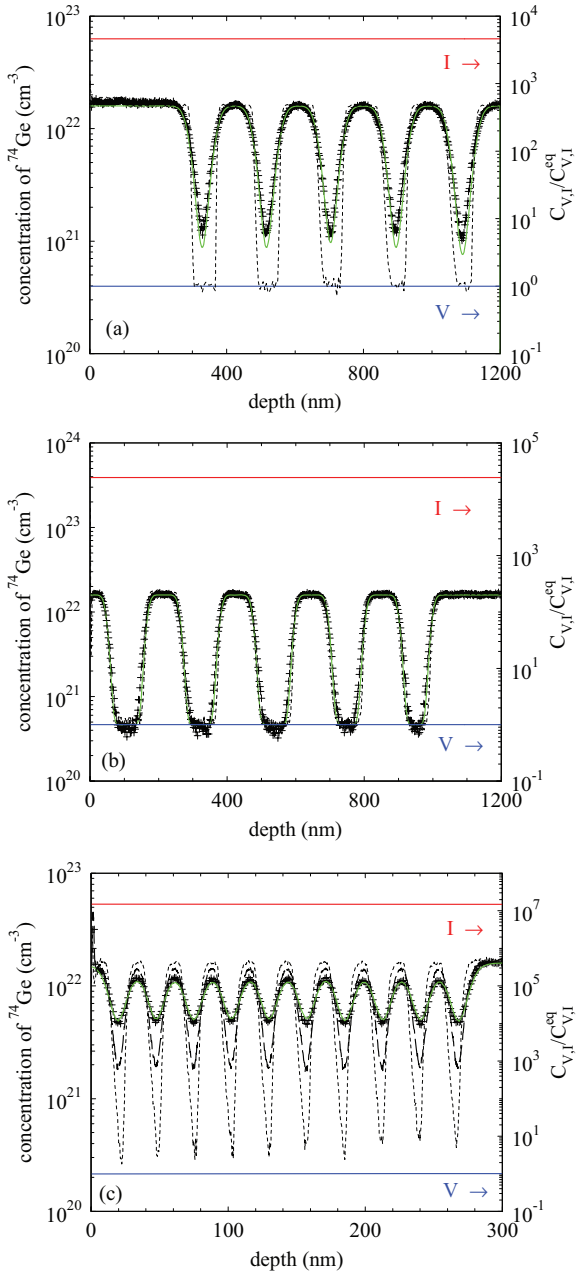

FIG. 2. (Color online) (a) Concentration profile of ^{74}Ge (+) of sample 1 measured with SIMS after annealing at 682 °C for 1800 s and concurrent irradiation with 2.5-MeV protons at a flux of 1.5 μA. (b) SIMS ^{74}Ge concentration profile (+) of sample 2 obtained after annealing at 660 °C for 900 s and concurrent irradiation with protons at a flux of 1.3 μA. (c) ^{74}Ge concentration profile (+) of sample 3 after concurrent annealing and proton irradiation at 587 °C for 5400 s with a proton flux of 1.0 μA. Solid lines in (a)–(c) represent best fits to the experimental ^{74}Ge profiles obtained on the basis of the model proposed in Sec. IV A for Ge self-diffusion under irradiation. The calculated normalized concentrations $C_{V,I}/C^{eq}_{V,I}$ of V and I are referred to the right axis. The distributions of both V and I are homogeneous with V concentrations in thermal equilibrium and I concentrations in high supersaturation. The short-dashed profiles in (a)–(c) show the ^{74}Ge profiles of the respective as-grown isotope structures. The long-dashed line in (c) represents the Ge profile beneath the covered part of the Ge sample that is not affected by proton irradiation during annealing.

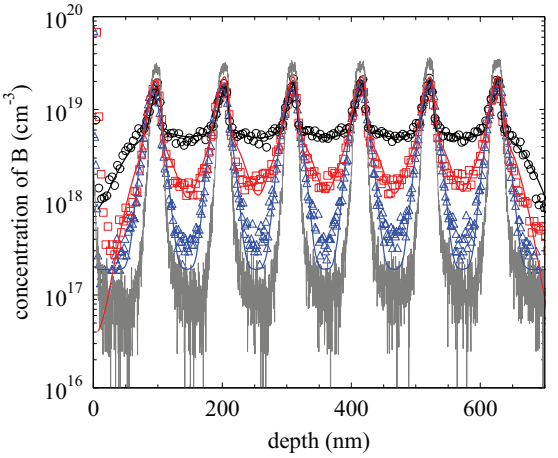

FIG. 3. (Color online) SIMS concentration profiles of B in Ge after concurrent annealing and irradiation (symbols) compared to the distribution of B in the as-grown structure (lower thin solid line). The profiles marked with blue triangle and red square represent B diffusion under irradiation at 630 °C and 550 °C, respectively, for 1 h and a proton flux of 1.5 μA. The B profiles reveal an atypical diffusion behavior under irradiation, i.e., stronger diffusional broadening of B at low compared to high temperatures. The upper profile (circle) obtained after concurrent annealing and irradiation at 570 °C for 3 h with a proton flux of 1.5 μA supports the presence of an immobile B fraction that adds to the total B profile measured with SIMS. The solid lines that reproduce the experimental B profiles are calculated on the basis of the B-diffusion model described in Sec. IV B. The model considers contributions of substitutional B_s, BI pairs, and immobile B clusters to the total B concentration measured with SIMS.

Solid lines in Figs. 2(a)–2(c) represent numerical simulations of self-diffusion under irradiation. The simulations consider the formation of Frenkel pairs due to irradiation, mutual annihilation of V and I in the bulk, and a limited annihilation efficiency at the surface. The accurate modeling of the experimental profiles supports the considered diffusion model, which is described together with its mathematical formulation in Sec. IV A.

B profiles measured after concurrent annealing and irradiation of sample No. 4 also reveal a homogeneous broadening as demonstrated by the profiles shown in Fig. 3. The homogeneous broadening is in compliance with the behavior of self-diffusion under irradiation. Moreover, the B profiles reveal an atypical diffusional broadening, i.e., a stronger broadening at low than at high temperatures and characteristic B spikes at the position of the original B-doped Ge layers that become apparent after diffusion at 570 °C for 3 h (see upper profile in Fig. 3). These B spikes are attributed to immobile B clusters that presumably are B-I clusters (BICs). However, the nature of the clusters still remains unsolved since we were not able to find any clusters by means of high-resolution TEM (HRTEM).

In the following, the diffusion of self- and B atoms in Ge under concurrent annealing and irradiation is described on the basis of appropriate atomic diffusion and defect reaction mechanisms. It is evidenced that the properties of Ge interstitials determine the characteristic diffusion behavior in Ge under proton irradiation.

IV. MODELING DIFFUSION UNDER IRRADIATION

A. Self-diffusion

Self-diffusion profiles established under irradiation and illustrated in Fig. 2 reveal an enhanced diffusion compared to thermal equilibrium [see Fig. 2(c)] but no significant depth-dependent broadening. Each profile indicates a constant depth-independent self-diffusion coefficient. Since self-diffusion in matter depends on both the concentration and mobility of native point defects,[35] the depth-independent self-diffusion reflects a homogeneous distribution of native point defects even under irradiation. A homogeneous distribution under irradiation is not expected in the case the Ge surface is an efficient sink for native defects. Hence, the annihilation of at least one type of native defect must be hindered. We propose that V readily annihilate at the surface, whereas I are reflected. This correlation is supported by the diffusion behavior of arsenic (As) in Ge. Under thermal equilibrium, As diffusion is mediated by V (Refs. 7 and 10) and under irradiation no significant enhancement of As diffusion is observed.[28,36] Obviously, the concentration of V under irradiation equals the concentration under thermal equilibrium. At first glance, this seems to be rather unlikely as irradiation continuously creates V and I. However, in the case the Ge surface acts as sink for V and reflects I, the disparity in the annihilation at the surface leads not only to a homogeneous distribution of V and I, but also to a strong I supersaturation and V concentrations close to thermal equilibrium. This is confirmed by numerical solutions of the following differential equations that describe Ge self-diffusion under *in situ* irradiation:

$$\frac{\partial C_V}{\partial t} - D_V \frac{\partial^2 C_V}{\partial x^2} = k_0 - k^+ C_V C_I + k^- C_0 C_0, \quad (1)$$

$$\frac{\partial C_I}{\partial t} - D_I \frac{\partial^2 C_I}{\partial x^2} = k_0 - k^+ C_V C_I + k^- C_0 C_0, \quad (2)$$

$$\frac{\partial C_{\mathrm{Ge}}}{\partial t} - \frac{\partial}{\partial x} D_{\mathrm{Ge}} \frac{\partial C_{\mathrm{Ge}}}{\partial x} = 0. \quad (3)$$

$C_{V,I,\mathrm{Ge}}$ and $D_{V,I,\mathrm{Ge}}$ are the concentrations of V, I, and ^{74}Ge as functions of depth and time and the corresponding diffusion coefficients, respectively. D_{Ge} is the self-diffusion coefficient of ^{74}Ge. Assuming a contribution of both V and I to self-diffusion, D_{Ge} is given by

$$\begin{aligned} D_{\mathrm{Ge}} &= (f_V C_V D_V + f_I C_I D_I)/C_0 \\ &= \left(f_V C_V^{\mathrm{eq}} D_V S_V + f_I C_I^{\mathrm{eq}} D_I S_I\right)/C_0 \\ &= f_V D_V^{\mathrm{SD}} S_V + f_I D_I^{\mathrm{SD}} S_I, \end{aligned} \quad (4)$$

where $S_{V,I} = C_{V,I}(x,t)/C_{V,I}^{\mathrm{eq}}$ represents the local concentration of V and I established under irradiation and normalized by the thermal equilibrium concentration $C_{V,I}^{\mathrm{eq}}$. $f_{V,I}$ is the diffusion correlation factor for self-diffusion via V and I. The values are set to $f_V = 0.5$ and $f_I = 0.56$ according to recent calculations on correlation effects of self-diffusion in diamond structures.[37,38] k_0 in Eqs. (1) and (2) is the production rate of V and I due to irradiation. This rate is equal for both native defects because V and I are created simultaneously. The parameter k_0 is proportional to the flux density and is considered to be constant across the entire isotope structure, in good agreement with binary collision simulations performed with SRIM.[33] For a specific proton flux, the generation rate k_0 is determined by the number of V-I pairs created by 2.5-MeV protons. Calculations with SRIM yield $k_0 = 2.3 \times 10^{-6}$ s^{-1} for a proton flux of 1 μA and an irradiated area of 0.785 cm^2. The term $k^+ C_V C_I$ describes the annihilation of V and I via the Frenkel pair reaction $I + V \rightleftharpoons 0$, where 0 reflects a Ge atom on a regular lattice site with an atom density of $C_0 = 4.413 \times 10^{22}$ cm^{-3}. The term $k^- C_0 C_0$ considers the thermal formation of V and I. Applying the law of mass action to the Frenkel pair reaction, the rate constants k^+ and k^- are interrelated via

$$\frac{k^+}{k^-} = \frac{C_0 C_0}{C_V^{\mathrm{eq}} C_I^{\mathrm{eq}}}. \quad (5)$$

This equation allows us to replace k^- in Eqs. (1) and (2) by $k^+ C_V^{\mathrm{eq}} C_I^{\mathrm{eq}}/(C_0 C_0)$. Assuming a diffusion-limited annihilation of V and I, k^+ is given by $4\pi r(D_V + D_I)$,[35] where r represents the capture radius. The capture radius is of the dimension of the Ge lattice constant ($a_0 = 5.6579$ Å) and set to $r = 0.5 \times a_0$. Equation (4) can be written in terms of the individual contributions $D_{V,I}^{\mathrm{SD}} = C_{V,I}^{\mathrm{eq}} D_{V,I}/C_0$ to the total Ge self-diffusion coefficient $D_{\mathrm{Ge}}^{\mathrm{SD}} = f_V D_V^{\mathrm{SD}} + f_I D_I^{\mathrm{SD}}$ under thermal equilibrium. $D_{\mathrm{Ge}}^{\mathrm{SD}}$ has been determined for temperatures between 429 °C and 904 °C.[6,16] The temperature dependence is accurately described with a single diffusion activation enthalpy of 3.13 eV and a preexponential factor of 25.4 cm^2 s^{-1}.[16] For the simulation of Ge self-diffusion under irradiation D_V^{SD} and D_I^{SD} are not independent, i.e., a variation of D_I^{SD} changes D_V^{SD} via $D_V^{\mathrm{SD}} = (D_{\mathrm{Ge}}^{\mathrm{SD}} - f_I D_I^{\mathrm{SD}})/f_V$. In this way, it is ensured that the sum of D_V^{SD} and D_I^{SD} equals the experimentally determined total self-diffusion coefficient under thermal equilibrium. The thermal equilibrium concentration of V is approximated by $C_V^{\mathrm{eq}}/C_0 \approx 2 \times 10^2 \exp(-1.97\ \mathrm{eV}/k_B T)$. This temperature dependence has been deduced by Vanhellemont *et al.*[24] from resistivity changes measured after quenching of Ge from high temperatures. For the analysis, the author considered isolated V to be responsible for the measured acceptor concentration. Accordingly, the temperature dependence of C_V^{eq} represents an upper bound since other defects may have contributed to the resistivity change. Different settings of C_V^{eq} under the constraint $C_V^{\mathrm{eq}} \gg C_I^{\mathrm{eq}}$ do not significantly affect the simulation result. This, in particular, holds as the boundary conditions assumed for V and I and expressed by

$$C_V(0,t) = C_V^{\mathrm{eq}}, \quad (6)$$

$$\left(\frac{\partial C_I}{\partial x}\right)_{(x=0,t)} = 0 \quad (7)$$

lead under steady-state conditions to a homogeneous distribution of V and I with $C_V(x,t) \approx C_V^{\mathrm{eq}}$ and $C_I(x,t) \gg C_I^{\mathrm{eq}}$ due to the disparity in the annihilation of V and I at the surface. As a consequence, Ge self-diffusion under irradiation is not sensitive to C_V^{eq}, C_I^{eq}, and D_I^{SD}, i.e., higher values assumed for C_I^{eq}/C_0 can be compensated by lower D_I^{SD} values. Mainly, the ratio $D_I^{\mathrm{SD}}/(C_I^{\mathrm{eq}}/C_0) = D_I$ determines self-diffusion of Ge under proton irradiation. For the temperature dependence of C_I^{eq}/C_0, we assume a prefactor of 2.4×10^6 and a formation enthalpy of 3.2 eV that is consistent with recent results of atomistic calculations.[20]

TABLE I. Diffusion coefficients of self-interstitials I in Ge deduced from self-diffusion experiments under proton irradiation with samples 1 to 3 at the temperatures T, times t, and proton fluxes Φ indicated.

Sample No.	T (°C)	t (min)	Φ (μA)	D_I (cm^2 s^{-1})
3	554	180	1.8	7.95×10^{-12}
3	587	90	1.0	7.36×10^{-12}
3	605	60	1.6	1.51×10^{-11}
3	607	60	2.5	9.81×10^{-12}
3	610	60	1.6	1.97×10^{-11}
3	612	30	1.5	1.28×10^{-11}
1	626	70	1.6	4.58×10^{-11}
2	660	15	1.3	7.01×10^{-11}
3	665	15	1.8	9.82×10^{-11}
1	682	30	1.5	1.60×10^{-10}

The experimental self-diffusion profiles illustrated in Fig. 2 are described by numerical solutions of Eqs. (1)–(3) with Eqs. (6) and (7) as boundary conditions. Thermal equilibrium of native point defects is assumed as initial condition for V and I. The respective as-grown ^{74}Ge profiles are considered as initial profiles. The V-related model parameters D_V and D_V^{SD} entering into Eqs. (1)–(4) are calculated via the relation assumed for C_V^{eq} (see above) and $D_V^{SD} = (D_{Ge}^{SD} - f_I D_I^{SD})/f_V$, respectively. Best fits to the experimental profiles illustrated in Fig. 2 were obtained with D_I as fitting parameter and the above-mentioned setting for C_I^{eq}/C_0. The data determined for D_I are listed in Table I and illustrated in Fig. 4 as function of the inverse temperature. The temperature dependence is best described by

$$D_I = 0.67^{+18.60}_{-0.64} \exp\left(-\frac{(1.84 \pm 0.26)\ \text{eV}}{k_B T}\right) \text{cm}^2\,\text{s}^{-1}. \quad (8)$$

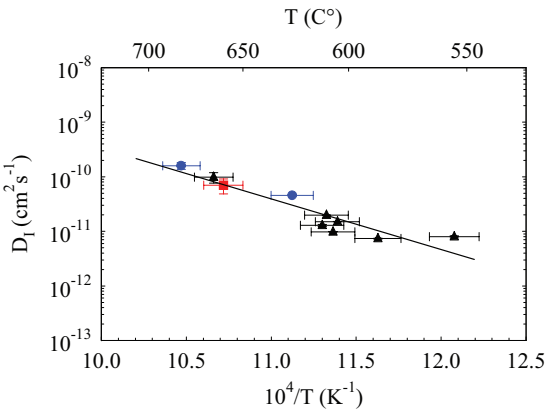

FIG. 4. (Color online) Diffusion coefficient D_I of self-interstitials in Ge vs the inverse temperature. The symbols blue dot, red square, and black triangle are data obtained from the analysis of Ge self-diffusion under proton irradiation utilizing samples 1, 2, and 3, respectively. The error mainly indicates the limited accuracy to determine the actual temperature of the Ge sample during concurrent annealing and irradiation. The temperature dependence is described by an Arrhenius equation [see Eq. (8)] with the diffusion activation enthalpy $Q = (1.84 \pm 0.26)$ eV and preexponential factor $D_o = (0.67^{+18.60}_{-0.64})$ cm^2 s^{-1}.

The scatter in the experimental data reflects the limited accuracy to determine both the actual temperature of the sample during irradiation and the proton beam current.

B. Boron diffusion

Experiments on the diffusion of B in Ge under thermal equilibrium conditions show a much slower mobility for B than for self-atoms.[7,16,39] The activation enthalpy of B diffusion exceeds with 4.65 eV (Ref. 39) clearly the value of 3.13 eV determined for self-diffusion.[16] The lower B diffusivity and higher activation enthalpy compared to self-diffusion led Uppal *et al.*[39] to propose that I rather than V mediate B diffusion in Ge. *Ab initio* investigations seem to support a B diffusion in Ge via an interstitialcy rather than a vacancy mechanism.[32] However, the calculated diffusion activation enthalpy for B diffusion via I (V) is significantly lower (higher) than the experimental result.[32] This demonstrates on one hand the difficulties of atomistic modeling methods to accurately predict the diffusion properties of dopants in semiconductors and on the other hand that a V-mediated diffusion of B can not be excluded, in particular, for thermal equilibrium conditions. In fact, the experimentally observed high activation enthalpy of B diffusion can be described with a V-mediated diffusion and a repulsive interaction between B and V. Atomistic calculations based on density functional theory confirm such repulsive interactions.[40,41] In contrast, under nonequilibrium conditions, i.e., experimental conditions that favor the formation of self-interstitials to concentrations that exceed the thermal equilibrium concentration by several orders of magnitude, diffusion of B can be mainly mediated by self-interstitials. A I- rather than V-mediated diffusion of B under irradiation is even more likely because under irradiation the V concentration in Ge is close to thermal equilibrium. This is a consequence of the disparity in the annihilation behavior of I and V at the Ge surface (see Sec. IV A). The absence of any radiation-enhanced diffusion of arsenic in Ge,[36] whose diffusion is mainly mediated by V,[7,10] and the heavily enhanced diffusion of B (Refs. 25, 26, and 28) demonstrates that the migration of B under irradiation can not be mediated by V. Accordingly, B diffusion in Ge under irradiation must be controlled by self-interstitials and the following defect reactions are considered for modeling its diffusion behavior:

$$(BI)^+ \leftrightharpoons B_s^- + I^{2+}, \quad (9)$$

$$(BI)^+ + V^{2-} \leftrightharpoons B_s^-, \quad (10)$$

$$I^{2+} + V^{2-} \leftrightharpoons 0. \quad (11)$$

Reaction (9) describes the formation of substitutional B_s and I via the dissociation of a BI pair. These pairs can be annihilated by means of V thereby forming B_s as expressed by reaction (10). Direct annihilation of I and V is considered by reaction (11). The reverse direction of reactions (9) to (11) characterize the conversion of B_s to mobile BI pairs and the formation of a Frenkel defect. The superscripts indicate the charge states assumed for the point defects. The single acceptor nature of B_s^- is generally accepted. Experiments on the simultaneous diffusion of n-type dopants and self-atoms demonstrate that

the vacancy in Ge is doubly negatively charged even under electronically intrinsic conditions.[8,9] Investigations of the electronic properties of defects in Ge resulting from electron irradiation reveal an acceptor energy level of 0.14 eV above the valence band and two donor states with energy positions of 0.08 and 0.24 eV below the conduction band of Ge.[42] The acceptor state is assigned to the $V^{2-/-}$ ionization level of the vacancy and the donor state at 0.08 eV (0.24 eV) to the ionization level of $I^{0/+}$ ($I^{+/2+}$).[42] Accordingly, the vacancy under p-type doping conditions is likely also negatively charged. A donor state for I in the upper half of the Ge band gap was also postulated from the trapping of point defects at radioactive ^{111}In probes studied by means of perturbed angular correlation spectroscopy.[43] In accord with these results, the vacancy (self-interstitial) is considered to be doubly negatively (positively) charged. In order to ensure charge neutrality of reactions (9) and (10), the BI pairs are assumed to be singly positively charged. The mathematical formulation of B diffusion based on reactions (9)–(11) is described by the following set of coupled partial differential equations:

$$\frac{\partial C_{\mathrm{B}_s^-}}{\partial t} = \frac{\partial}{\partial t}\left(D_{\mathrm{B}_s^-}\frac{\partial C_{\mathrm{B}_s^-}}{\partial x} + \frac{C_{\mathrm{B}_s^-}D_{\mathrm{B}_s^-}}{p(x)}\frac{\partial p(x)}{\partial x}\right) + k_1^+ C_{(\mathrm{B}I)^+}C_0 - k_1^- C_{\mathrm{B}_s^-}C_{I^{2+}} + k_2^+ C_{(\mathrm{B}I)^+}C_{V^{2-}} - k_2^- C_{\mathrm{B}_s^-}C_0, \tag{12}$$

$$\frac{\partial C_{I^{2+}}}{\partial t} = \frac{\partial}{\partial t}\left(D_I^{2+}\frac{\partial C_{I^{2+}}}{\partial x} - 2\frac{C_{I^{2+}}D_{I^{2+}}}{p(x)}\frac{\partial p(x)}{\partial x}\right) + k_0 + k_1^+ C_{(\mathrm{B}I)^+}C_0 - k_1^- C_{\mathrm{B}_s^-}C_{I^{2+}} - k^+ C_{I^{2+}}C_{V^{2-}} + k^- C_0 C_0, \tag{13}$$

$$\frac{\partial C_{V^{2-}}}{\partial t} = \frac{\partial}{\partial t}\left(D_V^{2-}\frac{\partial C_{V^{2-}}}{\partial x} + 2\frac{C_{V^{2-}}D_{V^{2-}}}{p(x)}\frac{\partial p(x)}{\partial x}\right) + k_0 - k_2^+ C_{(\mathrm{B}I)^+}C_{V^{2-}} + k_2^- C_{\mathrm{B}_s^-}C_0 - k^+ C_{I^{2+}}C_{V^{2-}} + k^- C_0 C_0, \tag{14}$$

$$\frac{\partial C_{(\mathrm{B}I)^+}}{\partial t} = \frac{\partial}{\partial t}\left(D_{(\mathrm{B}I)^+}\frac{\partial C_{(\mathrm{B}I)^+}}{\partial x} - \frac{C_{(\mathrm{B}I)^+}D_{(\mathrm{B}I)^+}}{p(x)}\frac{\partial p(x)}{\partial x}\right) - k_1^+ C_{(\mathrm{B}I)^+}C_0 + k_1^- C_{\mathrm{B}_s^-}C_{I^{2+}} - k_2^+ C_{(\mathrm{B}I)^+}C_{V^{2-}} + k_2^- C_{\mathrm{B}_s^-}C_0. \tag{15}$$

Again, C_X and D_X with $X \in \{\mathrm{B}_s^-, (\mathrm{B}I)^+, V^{2-}, I^{2+}\}$ are the concentrations and diffusion coefficients of the particular defects. The second term inside the brackets on the right-hand side of Eqs. (12)–(15) considers the possible impact of a built-in electric field on the diffusion of charged defects.[44] $p(x)$ is the free-hole concentration, which is determined by the concentration of the charged defects via the neutrality equation. Under electronic intrinsic conditions, the hole concentration equals to a good approximation the intrinsic carrier concentration n_i, i.e., $p(x) \approx n_i$, and thus $\partial p(x)/\partial x \approx 0$ holds. k_1^+ (k_2^+) and k_1^- (k_2^-) are, respectively, the forward and backward reaction constants of reaction (9) [reaction (10)]. Applying the law of mass action to reactions (9) and (10), the rate constants are interrelated via

$$\frac{k^{+1}}{k^{-1}} = \frac{C_{\mathrm{B}_s^-}^{\mathrm{eq}}C_{I^{2+}}^{\mathrm{eq}}}{C_{(\mathrm{B}I)^+}^{\mathrm{eq}}C_0}, \tag{16}$$

$$\frac{k^{+2}}{k^{-2}} = \frac{C_{\mathrm{B}_s^-}^{\mathrm{eq}}C_0}{C_{(\mathrm{B}I)^+}^{\mathrm{eq}}C_{V^{2-}}^{\mathrm{eq}}} \tag{17}$$

with the concentrations of the defects in thermal equilibrium. k_0 in Eqs. (13) and (14) accounts for the formation of V and I in equal numbers via proton irradiation. Equation (16) [Eq. (17)] is used to replace k_1^+ (k_2^-) in Eqs. (12), (13), and (15) [Eqs. (12), (14), and (15)] in terms of k_1^- (k_2^+). Assuming a diffusion-limited formation of BI pairs via reaction (9) and of B_s^- via reaction (10), the rate constants are given by

$$k_1^- = 4\pi r D_{I^{2+}}, \tag{18}$$

$$k_2^+ = 4\pi r (D_{(\mathrm{B}I)^+} + D_{V^{2-}}), \tag{19}$$

where r represents the capture radius. As in the case of self-diffusion (see Sec. IV A), the capture radius is set to $r = 0.5 \times a_0$. Equations (6), (7), and thermal equilibrium are assumed as boundary and initial conditions for V and I. The initial total concentration of B is set to the B profile of the as-grown structure measured with SIMS. The concentration of B_s^- is set to a maximum value of 5×10^{18} cm^{-3} because the diffusional broadening of the B-doped multilayer structure reveals the presence of immobile B spikes probably due to B clusters (see upper profile of Fig. 3). The initial concentration of BI pairs is adjusted to fulfill local equilibrium of reactions (9) and (10). Since the experimental B profiles measured after diffusion annealing do not reveal any significant dopant loss to the surface, reflecting boundary conditions are assumed for BI pairs and B_s. Data of B diffusion in Ge reported by Uppal *et al.*[39] are extrapolated to the temperatures used in this work and considered for the intrinsic B diffusion coefficient $D^*_{(\mathrm{B}I)^+} = C^{\mathrm{eq}}_{(\mathrm{B}I)^+}D_{(\mathrm{B}I)^+}/C^{\mathrm{eq}}_{\mathrm{B}_s^-}$ with $C^{\mathrm{eq}}_{\mathrm{B}_s^-} \approx 5 \times 10^{18}$ cm^{-3}. This implies that we consider an I-mediated B diffusion in Ge under thermal equilibrium although a V-mediated diffusion via the vacancy mechanism can, in principle, not be excluded (see above and discussion in Sec. V). The model parameter $D_{(\mathrm{B}I)^+}$ of Eq. (15) is expressed by $D_{(\mathrm{B}I)^+} = D^*_{(\mathrm{B}I)^+} \times C^{\mathrm{eq}}_{\mathrm{B}_s^-}/C^{\mathrm{eq}}_{(\mathrm{B}I)^+}$. Taking into account the I- and V-related parameters that model self-diffusion under irradiation, the quantity $C^{\mathrm{eq}}_{(\mathrm{B}I)^+}$ remains as free parameter to describe the experimental B profiles.

Numerical solutions of the differential equations (12)–(15) are shown by the solid lines in Figs. 3 and 5. Figure 3 demonstrates that the calculations accurately reproduce the atypical behavior of B diffusion under irradiation. This is illustrated by the stronger broadening of the B profiles at low temperatures (red square) compared to high temperatures (blue triangle) under otherwise identical irradiation conditions. The individual contributions to the total B diffusion profiles and the concentrations of I and V established under irradiation are illustrated in Figs. 5(a)–5(d). The total B concentration is given by contributions due to B_s, BI, and B atoms in clusters. The contribution of B clusters is evident by the spikes that remain after long diffusion times [see Fig. 5(c)]. Taking into account these immobile clusters, whose fraction to the total B concentration is described by Gaussian functions illustrated in Fig. 5 with slight variations in the maximum concentration of

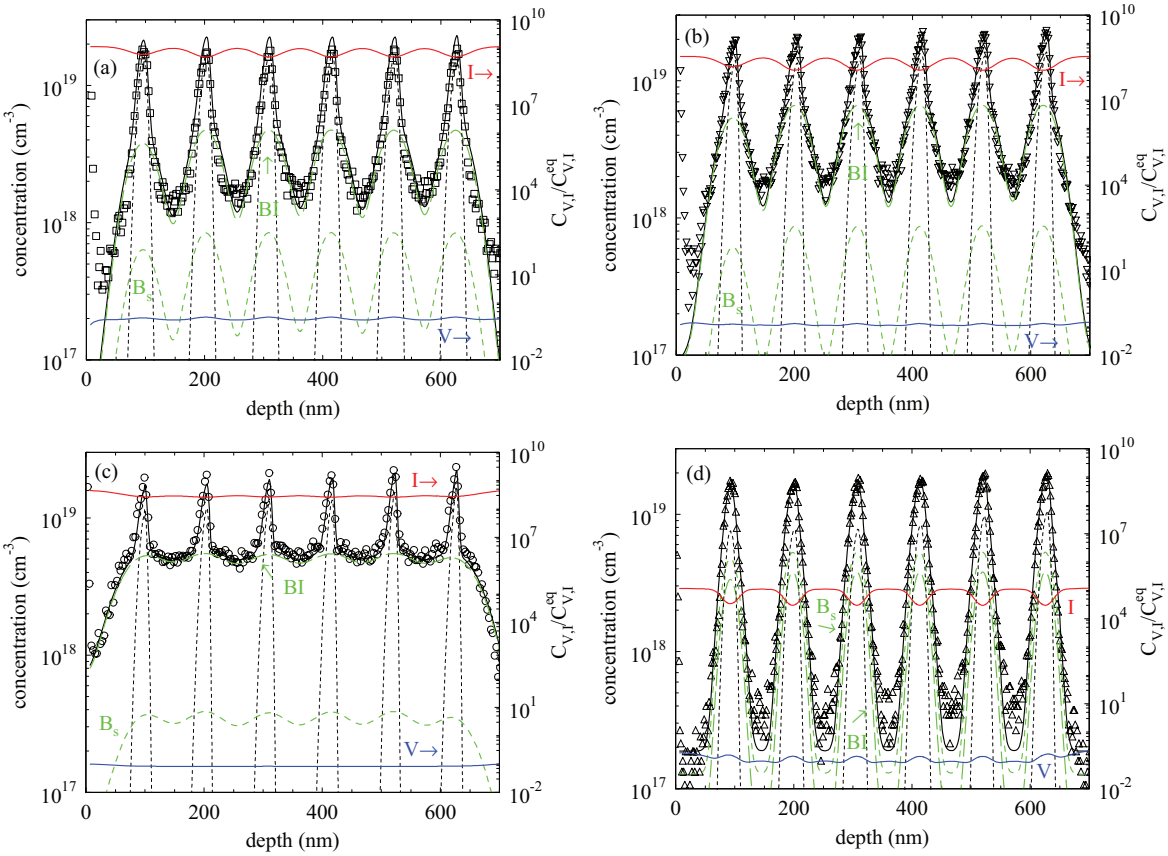

FIG. 5. (Color online) Concentration profiles of B (symbols) measured with SIMS after concurrent irradiation with 2.5-MeV protons at a flux of 1.5 μA and annealing at (a) 550 °C for 1 h, (b) 570 °C for 1 h, (c) 570 °C for 3 h, and (d) 630 °C for 1 h. The contributions of B_s (green short-dashed line), BI (green long-dashed line), and B aggregated in immobile clusters (black fine-dashed line) adds up to the total B concentration (black solid line). The calculated total B concentration accurately describes the experimental profile. The corresponding undersaturation and supersaturation of V and I are displayed by the blue and red solid lines, respectively. These profiles are referred to the right y axis.

the Gaussian peak,[45] the contributions of B_s and BI to the total B concentration are obtained by fitting numerical solutions of Eqs. (12)–(15) to the experimental B profiles with $C^{eq}_{(BI)^+}$ as free parameter. The values deduced for $C^{eq}_{(BI)^+}$ are listed in Table II and illustrated in Fig. 6 as function of the inverse temperature. The temperature dependence is best described by

$$C^{eq}_{(BI)^+} = 2.0 \times 10^{35} \left(^{+1.6\times10^{36}}_{-1.8\times10^{35}}\right) \times \exp\left(-\frac{(3.84 \pm 0.16)\ \text{eV}}{k_B T}\right) \text{cm}^{-3}. \quad (20)$$

TABLE II. Concentration $C^{eq}_{(BI)^+}$ of $(BI)^+$ pairs in thermal equilibrium determined from B-diffusion experiments under proton irradiation at the temperatures T, times t, and proton fluxes Φ indicated.

Sample No.	T (°C)	t (min)	Φ (μA)	$C^{eq}_{(BI)^+}$ (cm^{-3})
4	515	60	1.5	3.8×10^{10}
4	550	60	1.5	4.3×10^{11}
4	570	60	1.5	2.1×10^{12}
4	570	180	1.5	2.2×10^{12}
4	600	60	1.5	1.8×10^{13}
4	630	60	1.5	1.1×10^{14}
4	720	60	3.2	3.7×10^{15}

The scatter in the experimental data reflects the limited accuracy to determine the actual temperature of the sample during irradiation. For the range of temperatures studied in this work, the equilibrium concentration of BI pairs is well below the concentration of B_s ($C^{eq}_{B_s^-} = 5\times10^{18}$ cm^{-3}). Under proton irradiation, the concentration of I is highly supersaturated with

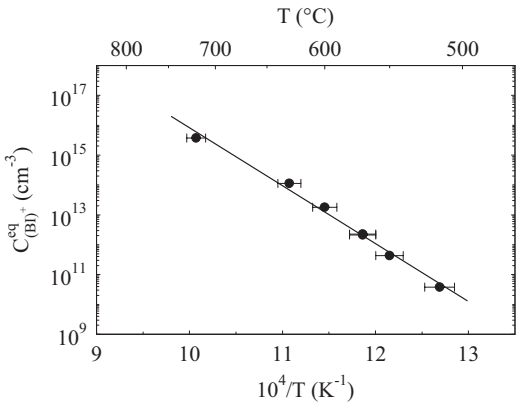

FIG. 6. Thermal equilibrium concentration $C^{eq}_{(BI)^+}$ of $(BI)^+$ pairs in Ge vs the inverse temperature. Data (symbols) were determined from modeling B diffusion in Ge under proton irradiation. The temperature dependence (solid line) is reproduced by Eq. (20).

respect to thermal equilibrium as illustrated in Figs. 5(a)–5(d). As a consequence, the concentration of BI under irradiation can exceed the concentration of B_s. This, in particular, holds for irradiations at low temperatures where a high-I supersaturation is favored due to a reduced I-V annihilation. The simulations illustrate that the enhanced diffusion of B with decreasing temperature is due to the formation of mobile BI pairs, whose concentration exceeds the concentration of B_s. The formation of BI pairs and their diffusion leads to a decrease of the I concentration within the B-doped Ge region [see I profiles shown in Figs. 5(a)–5(d)]. This is associated via Frenkel pair annihilation with a V concentration in the B-doped regions that exceeds the V concentration in regions outside of the B spikes.

V. DISCUSSION

The model proposed for the simulation of the self- and B diffusion in Ge under proton irradiation provides a consistent interpretation of the experimental diffusion profiles. The model parameters used for the simulation of self-diffusion were considered for modeling B diffusion. The observed behavior of self- and B diffusion in Ge under irradiation is strongly linked to the limited efficiency of the Ge surface to annihilate I. As a consequence, a high-I supersaturation is established whereas the V concentration stays close to thermal equilibrium. The I supersaturation favors the formation of mobile BI pairs, whose concentration exceeds the concentration of immobile B_s,[46] and leads to an enhanced B diffusion compared to thermal equilibrium conditions. Under constant irradiation conditions ($\Phi = 1.5\ \mu$A for $t = 60$ min) an increasing supersaturation of I with decreasing temperature evolves due to the decreasing I-V annihilation efficiency. This is experimentally reflected by the increasing diffusion of B under irradiation with decreasing temperature (see Fig. 3). Modeling of the experimental self- and B-atom profiles provides information about the migration enthalpy of I and formation enthalpy of BI pairs. The temperature dependence of D_I shown in Fig. 4 and given by Eq. (8) yields (1.84 ± 0.26) eV for the migration enthalpy of I. The preexponential factor $D_0 = (0.67^{+18.60}_{-0.64})\ \mathrm{cm^2 s^{-1}}$ is interrelated via $D_0 = g_I a_0^2 \nu_0 \exp(S_I^m/k_B)$ to the migration entropy $S_I^m \approx (4.4 \pm 3.4) k_B$ of I, in which $g_I = \frac{1}{4}$,[47] $\nu_0 \approx 10^{13}\ \mathrm{s^{-1}}$, and $a_0 = 5.6579$ Å are the geometry factor, attempt frequency (≈Debye frequency), and lattice constant, respectively. The temperature dependence deduced for the equilibrium concentration of $(BI)^+$ pairs yields $H^f_{(BI)^+} = (3.84 \pm 0.16)$ eV for the formation enthalpy of this defect. The preexponential factor equals $C_0 \exp(S^f_{(BI)^+}/k_B)$. With the Ge atom density of $C_0 = 4.413 \times 10^{22}\ \mathrm{cm^{-3}}$ a formation entropy $S^f_{(BI)^+} = (29 \pm 2) k_B$ is obtained. The high energy and entropy of BI formation is consistent with the slow diffusion of B in Ge under thermal equilibrium conditions.[39]

The data obtained for the enthalpy of I migration and BI formation can be compared with recent results of theoretical calculations. Carvalho *et al.*[30] determined by means of density functional theory the migration energies for Ge interstitials in various charge states. For neutral and singly positively charged Ge interstitials, a migration energy of 0.5 and 0.3 eV is predicted. A value of 1.2 eV was found for the migration energy of I^{2+}. This value is in acceptable agreement with the migration enthalpy of $H_I^m = (1.84 \pm 0.26)$ eV determined in this work for I. Consistently, the self-interstitials that mediate Ge self-diffusion under irradiation are concluded to be doubly positively charged. This is also supported by Haesslein *et al.*,[43] whose experiments reveal a donor state of I in the upper half of the Ge band gap. Consistently, the charge state of I has been considered for modeling the behavior of B diffusion under irradiation [see reactions (9) and (11)].

Delugas and Fiorentini[31] calculated via first-principles methods the formation enthalpy of both B interstitials and BI pairs. According to their calculations, the formation of BI is more favorable than the formation of B interstitials. For singly positively charged $(BI)^+$ pairs, formation energies between 2.77 and 3.04 eV depending on the position of the Fermi level are predicted. More recent theoretical investigations of Janke *et al.*[32] report formation energies between 2.5 and 3.0 eV for $(BI)^+$. However, the authors state that the disregard of electronic thermal excitations can cause corrections of ∼1 eV. In view of these uncertainties, an acceptable agreement is obtained for the formation energy of $(BI)^+$ pairs determined experimentally [(3.84±0.16) eV] and theoretically (2.5–3.0 eV). The overall consistency obtained by means of the proposed model to describe self- and B diffusion in Ge under irradiation supports an I-mediated diffusion of B under thermal equilibrium as already suggested by Uppal *et al.*[39]

Bruno *et al.*[26,27,29] report on experiments of B diffusion under proton irradiation for temperatures between −196 °C and 800 °C. The proton flux used in their experiments was about one-fifth of the flux used in this work. The authors confirm an enhanced diffusion of B and ascribe this to the formation of I that mediate B diffusion. A slight decrease in B diffusion with decreasing temperature between room temperature and 550 °C with an activation enthalpy of 0.1 eV is reported. No increasing diffusion with decreasing temperature is observed. Instead, a change in the shape of the B-diffusion profiles becomes evident. For temperatures above 750 °C, Gaussian-shaped profiles are observed, whereas for temperatures below 400 °C profiles with long exponential tails are obtained. This observation is neither consistent nor contradictory to our results because a direct comparison between the experiments performed by Bruno *et al.*[26,27,29] and those described in this work is difficult. Bruno *et al.* utilize H^+ ion implantation in relatively thick Ge samples rather than high-energy H^+ irradiation of thin Ge samples. Whereas H implantation in thick samples leads to end-of-range defects, the H^+ irradiation performed in this work leads to a penetration of H through the entire Ge sample (thinned to 30 μm) and a depth-independent formation of isolated Frenkel pairs. We ensured by means of transmission electron microscopy (TEM) that no extended defects were formed during the preparation of the thin Ge samples. Moreover, high-resolution TEM (HRTEM) of irradiated samples could not resolve any B clusters that are evident from the immobile part of the B profiles (see upper profile in Fig. 3). Presumably, these B clusters are too small to be detected by HRTEM or the part of the sample with clusters was missed in the preparation of samples for cross-section analysis. Nonetheless, the stability of the immobile B clusters under I supersaturation shows that the clusters likely consist of B-I clusters (BICs), whose

dissolution is hindered under I supersaturation. Such clusters are known to exist in Si (see, e.g., Ref. 48 and references therein) but have to the authors knowledge not yet been discovered in Ge. This demonstrates that the experimental conditions established by implantation on one hand and irradiation on the other hand are very different. In the case of H implantation, the kinetics of formation and dissolution of end-of-range defects mainly controls B diffusion, whereas in the case of H irradiation the diffusion of I and V and the kinetic of V-I annihilation mainly affects B diffusion. Nonetheless, the B diffusion study of Bruno *et al.*[26,27,29] demonstrates an enhanced B diffusion due to I. However, detailed information about the distribution, concentration, and properties of the individual defects involved in B diffusion and on the impact of the Ge surface are not accessible through their study in conjunction with the g/λ approach that was used for the analysis of the experimental profiles.

The defect reactions proposed in this work consistently explain the diffusion behavior of self- and B atoms in Ge. Moreover, the results are consistent with the diffusion of n-type dopants in Ge under irradiation.[36] The unusual behavior of Ge under irradiation is directly related to the limited efficiency of the Ge surface to annihilate Ge interstitials. This property of the Ge surface was postulated[25] in order to explain all experimental self- and dopant-atom diffusion profiles established under irradiation. To our understanding, no other mechanisms are able to explain the drastic disparity in the concentration of V and I under irradiation. Accordingly, understanding of the Ge surface property is the key to the strong I-V imbalance. Although the experiments performed so far are not able to decide on the mechanisms behind the limited I-annihilation efficiency of the Ge surface, the physical mechanism is likely related to Coulomb and/or elastic interactions. As discussed above, the self-interstitial in Ge is positively charged. On the other hand, electronic states established at the Ge surface or at interfaces are known to pin the Fermi level.[49] This is already known since the pioneering work of Brattain and Bardeen[50] on the Ge point contact transistor. The operation of the point contact transistor relied on the fact that surface acceptor states have pinned the Fermi level near the valence band. As a consequence, an inversion layer of holes is formed near the Ge surface. The electric field established within the inversion layer would attract rather than repel positively charged self-interstitials created athermally in the bulk by irradiation. However, a few years later, Clarke[51] reported that surface acceptor states can be removed by heating in vacuum. Following this line, it is possible that the conditions realized by concurrent annealing and proton irradiation at a vacuum pressure of $\leqslant 2 \times 10^{-5}$ mbar favor donor-type surface states rather than acceptor states. In this case, the electric field within the inversion layer would hinder positively charged self-interstitials to annihilate at the surface. On the other hand, self-interstitials approaching the Ge surface may also be repelled by a strain field close to the surface. Such a strain field should cause a higher formation enthalpy of I at the Ge surface compared to the bulk. Recent *ab initio* studies of Kamiyama *et al.*[52] report on lower formation energies of V and I at the surface of Si crystals compared to the bulk due to structural relaxation. No similar theoretical studies have been performed for Ge to the authors' knowledge. Certainly, atomistic calculations can help to understand the interaction between I and the Ge surface, but in the end experiments have to prove the concept.

VI. CONCLUSION

Experiments on self- and B diffusion in Ge under *in situ* proton irradiation reveal enhanced diffusion compared to thermal equilibrium conditions. An accurate description of the experimental diffusion profiles is achieved on the basis of the Frenkel pair reaction and the dissociative and interstitialcy mechanisms of B diffusion. Thereby, the Ge surface is considered to be an efficient sink for vacancies but not for self-interstitials. The disparity in the annihilation of native point defects at the Ge surface leads to homogeneous, high concentrations of self-interstitials, which exceed their thermal equilibrium concentration by several orders of magnitude, and to homogeneous concentrations of vacancies close to thermal equilibrium. The unusual Ge surface property becomes evident by a depth-independent self- and B diffusion and an atypical B diffusion behavior that increases with decreasing temperature under otherwise same irradiation conditions. Comprehensive modeling of self- and B diffusion under irradiation is achieved on the basis of a common set of model parameters. The experimental diffusion profiles are reproduced by numerical simulations that consider the diffusion coefficient of doubly positively charged self-interstitials (I^{2+}) and the thermal equilibrium concentration of singly positively charged $(BI)^+$ pairs as free parameters. Best fits provide data for these two quantities. From their temperature dependence, the migration enthalpy $H^m_{I^{2+}} = (1.84 \pm 0.28)$ eV of I^{2+} and formation enthalpy $H^f_{(BI)^+} = (3.84 \pm 0.16)$ eV of $(BI)^+$ pairs in Ge is obtained. Theoretical calculations support I^{2+} and $(BI)^+$ pairs with thermodynamic properties in acceptable agreement with our results. The overall consistency of the diffusion model proposed to explain self- and dopant diffusion in Ge under concurrent annealing and irradiation supports the assumption that B diffuses via an I-mediate diffusion mechanisms even under thermal equilibrium conditions. The presence of B-I clusters (BICs) is concluded indirectly from the immobile fraction of the B profiles. These clusters are hindered to dissolve under irradiation due to the strong I supersaturation. The limited efficiency of the Ge surface to annihilate self-interstitials is the key for the unusual diffusion behavior of self- and B atoms in Ge under irradiation. This could be related to donor-type Ge surface states which are favored under vacuum conditions. The understanding of this surface phenomena will help to design strategies for controlling diffusion, doping, and defect reactions in Ge.

ACKNOWLEDGMENTS

The authors thank TASCON GmbH in Münster for the SIMS measurements. This work was funded by the Deutsche Forschungsgemeinschaft under Grants No. BR 1520/6-2 and No. SFB631 TPC4 as well as an individual grant within the Heisenberg program for H.B. The isotopically enriched Ge was developed with funding by the Director, Office of Science, Office of Basic Energy Sciences, Materials Sciences and Engineering Division, of the US DOE under Contract No. DE-AC02-05CH11231.

*bracht@uni-muenster.de

[1] *Germanium-Based Technologies–From Materials to Devices*, edited by C. Claeys and E. Simoen (Elsevier, Amsterdam, 2007).

[2] D. P. Brunco *et al.*, J. Electrochem. Soc. **155**, H552 (2008).

[3] E. Simoen, J. Mitard, G. Hellings, G. Eneman, B. De Jaeger, L. Witters, B. Vincent, R. Loo, A. Delabie, S. Sioncke, M. Caymax, and C. Claeys, Mater. Sci. Semicond. Process. **15**, 588 (2012).

[4] S. M. Sze, *Physics of Semiconductor Devices* (Wiley, New York, 2001).

[5] H. Bracht, H. H. Silvestri, I. D. Sharp, and E. E. Haller, Phys. Rev. B **75**, 035211 (2007).

[6] M. Werner, H. Mehrer, and H. D. Hochheimer, Phys. Rev. B **32**, 3930 (1985).

[7] H. Bracht and S. Brotzmann, Mater. Sci. Semicond. Process. **9**, 471 (2006).

[8] S. Brotzmann, H. Bracht, J. L. Hansen, A. N. Larsen, E. Simoen, E. E. Haller, J. S. Christensen, and P. Werner, Phys. Rev. B **77**, 235207 (2008).

[9] M. Naganawa, Y. Shimizu, M. Uematsu, K. M. Itoh, K. Sawano, Y. Shiraki, and E. E. Haller, Appl. Phys. Lett. **93**, 191905 (2008).

[10] S. Brotzmann and H. Bracht, J. Appl. Phys. **103**, 033508 (2008).

[11] P. Dorner, W. Gust, A. Lodding, H. Odelius, B. Predel, and U. Roll, Acta Metall. **30**, 941 (1982).

[12] P. Dorner, W. Gust, A. Lodding, H. Odelius, B. Predel, and U. Roll, Z. Metallkde. **73**, 325 (1982).

[13] U. Södervall, H. Odelius, A. Lodding, U. Roll, B. Predel, W. Gust, and P. Dorner, Philos. Mag. A **54**, 539 (1986).

[14] I. Riihimäki, A. Virtanen, S. Rinta-Anttila, P. Pusa, J. Räisänen (ISOLDE Collaboration), Appl. Phys. Lett. **91**, 091922 (2007).

[15] R. Kube, H. Bracht, A. Chroneos, M. Posselt, and B. Schmidt, J. Appl. Phys. **106**, 063534 (2009).

[16] E. Hüger, U. Tietze, D. Lott, H. Bracht, D. Bougeard, E. E. Haller, and H. Schmidt, Appl. Phys. Lett. **93**, 162104 (2008).

[17] A. Fazzio, A. Janotti, A. J. R. da Silva, and R. Mota, Phys. Rev. B **61**, R2401 (2000).

[18] A. J. R. da Silva, A. Janotti, A. Fazzio, R. J. Baierle, and R. Mota, Phys. Rev. B **62**, 9903 (2000).

[19] M. D. Moreira, R. H. Miwa, and P. Venezuela, Phys. Rev. B **70**, 115215 (2004).

[20] J. Vanhellemont, P. Śpiewak, and K. Sueoka, J. Appl. Phys. **101**, 036103 (2007).

[21] J. Vanhellemont and E. Simoen, J. Electrochem. Soc. **154**, H572 (2007).

[22] P. Śpiewak, J. Vanhellemont, K. Sueoka, K. J. Kurzydłowski, and I. Romandic, J. Appl. Phys. **103**, 086103 (2008).

[23] P. Śpiewak, J. Vanhellemont, K. Sueokad, K. J. Kurzydłowskia, and I. Romandic, Mater. Sci. Semicond. Process. **11**, 328 (2008).

[24] J. Vanhellemont, J. Lauwaert, A. Witecka, P. Śpiewak, I. Romandic, and P. Clauws, Phys. B (Amsterdam) **404**, 4529 (2009).

[25] H. Bracht, S. Schneider, J. N. Klug, C. Y. Liao, J. L. Hansen, E. E. Haller, A. N. Larsen, D. Bougeard, M. Posselt, and C. Wündisch, Phys. Rev. Lett. **103**, 255501 (2009).

[26] E. Bruno, S. Mirabella, G. Scapellato, G. Impellizzeri, A. Terrasi, F. Priolo, E. Napolitani, D. De Salvador, M. Mastromatteo, and A. Carnera, Phys. Rev. B **80**, 033204 (2009).

[27] E. Napolitani, G. Bisognin, E. Bruno, M. Mastromatteo, G. G. Scapellato, S. Boninelli, D. De Salvador, S. Mirabella, C. Spinella, A. Carnera, and F. Priolo, Appl. Phys. Lett. **96**, 201906 (2010).

[28] H. Bracht, S. Schneider, and R. Kube, Microelectron. Eng. **88**, 452 (2011).

[29] G. G. Scapellato, E. Bruno, A. J. Smith, E. Napolitani, D. De Salvador, S. Mirabella, M. Mastromatteo, A. Carnera, R. Gwilliam, and F. Priolo, Nucl. Instrum. Methods Phys. Res., Sect. B **282**, 8 (2012).

[30] A. Carvalho, R. Jones, C. Janke, J. P. Goss, P. R. Briddon, J. Coutinho, and S. Öberg, Phys. Rev. Lett. **99**, 175502 (2007).

[31] P. Delugas and V. Fiorentini, Phys. Rev. B **69**, 085203 (2004).

[32] C. Janke, R. Jones, S. Öberg, and P. R. Briddon, Phys. Rev. B **77**, 075208 (2008).

[33] J. P. Biersack and L. G. Haggmark, Nucl. Instrum. Methods **174**, 257 (1980).

[34] H. Bracht, J. F. Pedersen, N. Zangenberg, A. N. Larsen, E. E. Haller, G. Lulli, and M. Posselt, Phys. Rev. Lett. **91**, 245502 (2003).

[35] A. C. Damask and G. J. Dienes, *Point Defects in Metals* (Gordon and Breach, New York, 1963).

[36] S. Schneider and H. Bracht, Appl. Phys. Lett. **98**, 014101 (2011).

[37] M. Posselt, F. Gao, and D. Zwicker, Phys. Rev. B **71**, 245202 (2005).

[38] M. Posselt, F. Gao, and H. Bracht, Phys. Rev. B **78**, 035208 (2008).

[39] S. Uppal, A. F. W. Willoughby, J. M. Bonar, N. E. B. Cowern, T. Grasby, R. J. H. Morris, and M. G. Dowsett, J. Appl. Phys. **96**, 1376 (2004).

[40] A. Chroneos, B. P. Uberuaga, and R. W. Grimes, J. Appl. Phys. **102**, 083707 (2007).

[41] A. Chroneos, J. Appl. Phys. **107**, 076102 (2010).

[42] A. Mesli, L. Dobaczewski, K. B. Nielsen, V. Kolkovsky, M. C. Petersen, and A. N. Larsen, Phys. Rev. B **78**, 165202 (2008).

[43] H. Haesslein, R. Sielemann, and C. Zistl, Phys. Rev. Lett. **80**, 2626 (1998).

[44] H. Bracht, Phys. Rev. B **75**, 035210 (2007).

[45] The maximum peak concentration decreases with increasing temperature and remains within an accuracy of 20% constant at a given temperature. This indicates that the B clusters tend to dissolve with increasing temperature but still remain fairly stable for given temperature and irradiation conditions. The uncertainty due to B clusters does not significantly alter the main results of our simulations since their contribution to the total B profile stays approximately constant and can be fairly well extracted from the B profile shown in Fig. 5(c).

[46] Substitutional B_s is virtually immobile compared to the diffusion of B via BV and BI pairs. For our simulations of B diffusion under irradiation, the diffusion coefficient of B_s^- [see Eq. (12)] is assumed to $D_{B_s^-} \approx 0$.

[47] A. Seeger, H. Föll, and W. Frank, *Radiation Effects in Semiconductors 1976*, IOP Conf. Proc. No. 31 (Institute of Physics, London, 1977), p. 12.

[48] S. Mirabella, D. De Salvador, E. Napolitani, E. Bruno, and F. Priolo, J. Appl. Phys. **113**, 031101 (2013).

[49] A. Dimoulas and P. Tsipas, Microelectron. Eng. **86**, 1577 (2009).

[50] W. Brattain and J. Bardeen, Phys. Rev. **74**, 231 (1948).

[51] E. N. Clarke, Phys. Rev. **95**, 284 (1954).

[52] E. Kamiyama, K. Sueoka, and J. Vanhellemont, J. Appl. Phys. **111**, 083507 (2012).